PROCEEDINGS OF THE ROYAL SOCIETY B

rspb.royalsocietypublishing.org

Research

Cite this article: Zlatkina V, Petrides M. 2014 Morphological patterns of the intraparietal sulcus and the anterior intermediate parietal sulcus of Jensen in the human brain. *Proc. R. Soc. B* **281**: 20141493.
http://dx.doi.org/10.1098/rspb.2014.1493

Received: 27 June 2014
Accepted: 7 October 2014

Subject Areas:
neuroscience

Keywords:
sulcal morphology, MRI, area AIP, area LIP, area CIP, PRR

Author for correspondence:
Veronika Zlatkina
e-mail: veronika.zlatkina@mail.mcgill.ca

Electronic supplementary material is available at http://dx.doi.org/10.1098/rspb.2014.1493 or via http://rspb.royalsocietypublishing.org.

Royal Society Publishing

Morphological patterns of the intraparietal sulcus and the anterior intermediate parietal sulcus of Jensen in the human brain

Veronika Zlatkina and Michael Petrides

Montreal Neurological Institute, McGill University, Montreal, Quebec, Canada H3A 2B4

Distinct parts of the intraparietal sulcal cortex contribute to sensorimotor integration and visual spatial attentional processing. A detailed examination of the morphological relations of the different segments of the complex intraparietal sulcal region in the human brain in standard stereotaxic space, which is a prerequisite for detailed structure-to-function studies, is not available. This study examined the intraparietal sulcus (IPS) and the related sulcus of Jensen in magnetic resonance imaging brain volumes registered in the Montreal Neurological Institute stereotaxic space. It was demonstrated that the IPS is divided into two branches: the anterior ramus and the posterior ramus of the IPS, often separated by a submerged gyral passage. The sulcus of Jensen emerges between the anterior and posterior rami of the IPS, and its ventral end is positioned between the first and second caudal branches of the superior temporal sulcus. In a small number of brains, the sulcus of Jensen may merge superficially with the first caudal branch of the superior temporal sulcus. The above morphological findings are discussed in relation to previously reported functional neuroimaging findings and provide the basis for future exploration of structure-to-function relations in the posterior parietal region of individual subjects.

1. Introduction

The intraparietal sulcus (IPS), the main sulcus on the lateral surface of the posterior parietal lobe, was first described in the middle of the nineteenth century by Turner [1]. In the human brain, it is a complex sulcus and its functional organization is not well understood. By contrast, in the monkey, it is a relatively simple furrow and its functional organization has been clarified by elegant single-neuron recording studies. The anterior intraparietal sulcal cortex (area AIP) has been shown to be involved in complex sensorimotor integration [2–5], whereas its more central and caudal parts (lateral, medial and caudal intraparietal areas) play critical roles in visuospatial and attentional processing [6–15]. More recently, there have been several attempts to explore the functional organization of the intraparietal sulcal cortex in the human brain using functional neuroimaging methods [16–24] (for reviews, see [25–27]). Such studies face a major problem, namely the fact that, in the human brain, the sulcal segments of the IPS exhibit considerable variability. It is clear that understanding the morphological variability and relationships between the various intraparietal segments and the patterns formed with the nearby sulci is critical for detailed exploration of structure-to-function relations in the parietal region of the human brain, especially in individual brains. Several studies have now demonstrated that detailed understanding of the local sulcal morphology and its variability across brains is a prerequisite for the establishment of precise relations between cortical representations and the specific sulcal anatomy in individual subjects [28–30]. Structure-to-function relations that remained obscure from functional neuroimaging studies reporting only the average location of functional activity in standard stereotaxic space were uncovered

when activity was examined in individual subjects following a detailed understanding of the local morphological variability [28–30].

Although the IPS is frequently represented diagrammatically as a single continuous horizontally oriented sulcus, even a brief examination of the posterior parietal region in the human brain reveals a collection of sulci of varying lengths and orientations, indicating that the IPS is a complex of sulcal segments [31–34]. Furthermore, there is a poorly studied short sulcus: the anterior intermediate parietal sulcus of Jensen [34], also referred to as the sulcus intermedius [35] or sulcus intermedius primus of Jensen [36], which appears to emerge out of the inferior bank of the IPS and may have important functional implications. The limited information available about the structure of the IPS complex and its interindividual variability, as well as the sulcus of Jensen, is based on visual inspection of the sulci on the surface of the brain [37]. In order to advance understanding of the IPS patterns, it is necessary to examine the depth of the sulci in a continuous series of two-dimensional sections. Such an approach reveals discontinuities by gyral passages located in the sulcal depth, and therefore not visible from surface inspection of the brains [38]. This study examined the morphology of the intraparietal sulcal region in continuous serial two-dimensional sections in order to establish the details of the morphological variations of the IPS and clarify the relationship between its segments, the sulcus of Jensen and the nearby sulci, such as the three caudal branches of the superior temporal sulcus that enter the inferior parietal lobule and approach the IPS. The magnetic resonance imaging (MRI) brain volumes used were registered in the Montreal Neurological Institute (MNI) proportional stereotaxic space, which is the most frequently used framework to describe the location of structural and functional neuroimaging findings.

2. Methods

The methodology is similar to that in the study by Zlatkina & Petrides [38]. The data are based entirely on the examination of continuous series of sections in the region of interest. The three-dimensional surface reconstructions provided in this article are examples of a small number of cases in which the submerged gyral passages were large enough to be visualized by 'inflating' the brain volumes and, as such, could be used to provide the reader with the outward appearance of these discontinuities that are most often found in the depth of the IPS. Note also that the paroccipital sulcus, which is sometimes discussed in relation to the IPS, is not examined in this study as it is considered an independent sulcus found in the occipital region of the brain [34].

(a) Subjects

The sample consisted of 24 male (mean age 23.3 years, SD 4.05) and 16 female (mean age 24.6 years, SD 5.6) MRI brain volumes obtained from the International Consortium for Brain Mapping (ICBM) database (www.loni.usc.edu/ICBM) [39–41]. The ICBM project, which is supported by the National Institute of Biomedical Imaging and Bioengineering, is the result of efforts of co-investigators from University of California, Los Angeles (UCLA), MNI, University of Texas at San Antonio and the Institute of Medicine, Juelich/Heinrich Heine University—Germany. The identification numbers of the brain volumes used in this article are the following: mni_0100–mni_0103, mni_0107–mni_0112, mni_0114–mni_0121, mni_0123, mni_0125, mni_0131, mni_0133, mni_0135, mni_0137–mni_0141, mni_0144, mni_0146, mni_0148–mni_0153, mni_0200, mni_0201, mni_0203, mni_0204.

(b) Magnetic resonance imaging

The MRI scans were performed on a Philips gyroscan 1.5T superconducting magnet system. A three-dimensional spoiled gradient echo acquisition sequence was used to collect 178 contiguous sagittal T_1-weighted images (TR = 18 ms, TE = 10 ms, flip angle = 30°, 256 × 256 matrix, 256 mm FOV, voxel size isotropic 1 mm^3) covering the head from ear to ear. The intensity correction for non-uniformity was performed with the help of the N3 program [42]. The MRITOTAL program from the mni_autoreg package was applied to estimate the nine parameter linear transformation required to map the MRI data into the MNI stereotaxic space [43]. Each MRI volume was resampled using a trilinear kernel onto a 1 mm grid in the stereotaxic space.

(c) Segmentation of intrasulcal grey matter and surface renderings

The post-central sulcus, the IPS, the anterior intermediate parietal sulcus of Jensen, the sulcus of Brissaud and the paroccipital sulcus were identified and traced manually on individual MRI brain volumes with the help of an interactive imaging software package called DISPLAY [44]. The sulci of interest were examined in coronal, horizontal and sagittal sections at 1 mm intervals in order to determine their direction, extent and patterns formed with each other.

Three-dimensional surface renderings of individual brains were acquired using two different types of software. CIVET IMAGE PROCESSING PIPELINE v. 1.1.12, available via the CBRAIN interface (http://mcin-cnim.ca/neuroimagingtechnologies/cbrain/), was used to extract the cortical surfaces from the MINC files containing the individual MRI brain scans [45]. Additionally, CARET v. 5.5 software, available at http://brainvis.wustl.edu, was used to produce three-dimensional reconstructions of the same individual brains and slightly 'inflate' them (two smoothing iterations, inflation factor equal to 1) to reveal the deep or submerged parts of sulci, not commonly seen from the surface of the brain [46].

(d) Conversion of stereotaxic space coordinates

In some of the functional neuroimaging studies, Talairach & Tournoux [47] stereotaxic space coordinates were provided rather than MNI coordinates. In these cases, the Talairach and Tournoux coordinates were converted to MNI space coordinates using the signed differential method provided at http://www.sdmproject.com. The obtained MNI space coordinates of the region of interest were projected onto an average brain template (ICBM152 nonlinear sixth-generation model available from http://www.bic.mni.mcgill.ca [48]).

3. Results

It is important to note that, in this article, the IPS does not include the paroccipital sulcus, which is an independent sulcus that has sometimes been referred to as a posterior extension of the IPS (see [34]).

(a) Rami of the intraparietal sulcus and their connection with the paroccipital sulcus

The IPS extends posterior to the post-central sulcal complex as far as the sulcus of Brissaud and the anterior part of the paroccipital sulcus (figure 1). Investigation of the IPS in

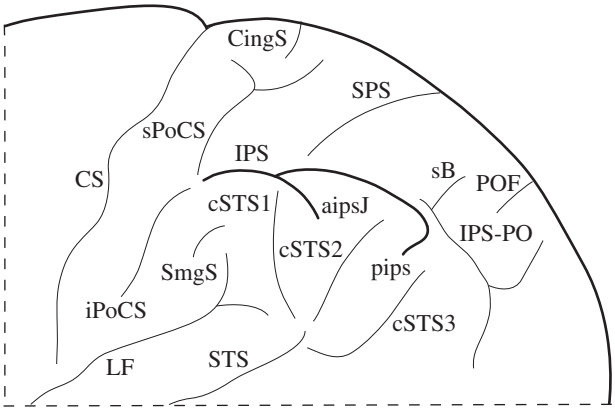

Figure 1. Schematic of the parietal sulci of interest on the lateral surface of the human brain. aipsJ, anterior intermediate parietal sulcus of Jensen; CingS, marginal branch of the cingulate sulcus on the lateral surface of the brain; CS, central sulcus; cSTS1, first caudal branch of the superior temporal sulcus; cSTS2, second caudal branch of the superior temporal sulcus; cSTS3, third caudal branch of the superior temporal sulcus; iPoCS, inferior branch of the post-central sulcus; IPS, intraparietal sulcus (main horizontal part of the intraparietal sulcus); IPS-PO, paroccipital sulcus, often considered as the paroccipital part of the intraparietal sulcus; LF, lateral fissure; pips, posterior intermediate parietal sulcus; POF, parietooccipital fissure; sB, sulcus of Brissaud; SmgS, supramarginal sulcus; sPoCS, superior branch of the post-central sulcus; SPS, superior parietal sulcus; STS, superior temporal sulcus.

continuous serial two-dimensional sections demonstrated that, in the majority of hemispheres, it could be divided, by a gyral passage, into two main branches: the anterior ramus and the posterior ramus (60% of the left hemispheres and 67.5% of the right hemispheres; figures 2*b–d*, 3; electronic supplementary material, figures S1*b*,*d*, S2, S4). This gyral passage is either submerged (figures 2*b*,*c*, 3*a*; electronic supplementary material, figures S1*d*, S2, S4) or visible from the surface of the brain (figure 2*d*). Much less frequently, the IPS was composed of three rami (10% of the left hemispheres and 7.5% of the right hemispheres). In a number of cases, the subdivisions of the IPS could not be determined and it was therefore treated as a single uninterrupted sulcus (30% of the left hemispheres and 25% of the right hemispheres; figure 2*a*; electronic supplementary material, figures S1*a*,*c*,*e*, S5–S8).

In general, the gyral passages separating the IPS into rami by linking its banks were most frequently submerged and not visible from the reconstructed brain surface (84.4% of all passages in the left and 63.6% of all passages in the right hemisphere; figure 3*a*; electronic supplementary material, figure S1*d*, S4). When present, these submerged gyral passages were generally more pronounced on the inferior bank of the IPS in close proximity to the dorsal terminations of the caudal superior temporal sulcus (electronic supplementary material, figure S2). In a smaller proportion of cases, the gyral passages were of considerable size and connected the banks of the IPS from the fundus to the surface, resulting in several disconnected and isolated sulcal units (15.6% of all passages in the left and 36.4% of all passages in the right hemisphere; figure 2*d*).

In 50% of the left hemispheres and 65% of the right hemispheres, the posterior end of the IPS was separated from the paroccipital sulcus by a gyral passage visible from the reconstructed brain surface (figure 2*a*,*b*; electronic supplementary material, figure S1*b*,*e*). In the remainder of the hemispheres, the posterior part of the IPS appeared to merge with the paroccipital sulcus on the surface of the brain, but these two sulci were still separated by a small gyral passage in the sulcal depth (figure 3*a–c*; the electronic supplementary material, figure S4). Superficial connection between the posterior ramus of the IPS and the paroccipital sulcus was sometimes completed with the help of a small tertiary sulcus (15% of the left and 7.5% of the right hemispheres).

A previous investigation of the IPS complex from the surface of the brain by Ono *et al.* [37] reported that the IPS complex is continuous in 72% of the left and 28% of the right hemispheres, and it is separated into two segments in 28% of the left and 68% of the right hemispheres [37, p. 67]. However, it should be noted that the two segments in the Ono *et al.* study [37] refer to the IPS proper (examined here) and the paroccipital sulcus, an independent sulcus that is sometimes treated as a component of the IPS complex. Thus, the two rami of the IPS reported here (and their percentages) refer to the IPS proper and not the IPS and the paroccipital sulcus.

The supramarginal sulcus was observed in the majority of left and right hemispheres on the supramarginal gyrus (87.5% of the left and 85% of the right hemispheres). It was either present as a set of dimples or a slightly more pronounced sulcus (figures 2, 3*a–c*; electronic supplementary material, figures S1, S4, S5, S7).

(b) Anterior intermediate parietal sulcus of Jensen

The anterior intermediate parietal sulcus of Jensen (also the sulcus of Jensen) is a short sulcus which emerges out of the inferior bank of the IPS at the posterior end of the supramarginal gyrus. Systematic examination of continuous serial two-dimensional sections demonstrated the sulcus of Jensen in 67.5% of the left and 80% of the right hemispheres.

In 40% of the left and 70% of the right hemispheres examined, the sulcus of Jensen emerged from the main stem of the IPS as a deep inferiorly directed side branch with no separation between the main stem and the side branch (i.e. with no gyral passage separating them; figure 2*a*; electronic supplementary material, figures S1*a*, S3*a*). In cases in which the sulcus of Jensen was underdeveloped, it appeared as a notch on the surface of the brain (12.5% of the left and 5% of the right hemispheres; figure 2*b*; electronic supplementary material, figures S1*b*, S3*b*).

In a smaller number of cases, the sulcus of Jensen consisted of a shallow sulcus attached to the main stem of the IPS, and the connection between the two sulci was observed in a number of horizontal sections (15% of the left and 5% of the right hemispheres; figures 2*c*, 3; electronic supplementary material, figures S1*c*,*d*, S3*c*, S4–S8).

Frequently, the sulcus of Jensen was located between the first and second caudal branches of the superior temporal sulcus (57.5% of the left and 62.5% of the right hemispheres; figure 2*a–c*; electronic supplementary material, figures S1*a–d*, S3*a–c*). In a smaller number of cases, the sulcus of Jensen merged superficially with the first caudal branch of the superior temporal sulcus (7.5% of the left and 17.5% of the right hemispheres; figure 2*d*; electronic supplementary material, figures S1*e*, S3*d*). However, the two sulci were separated in the depth by a submerged gyral passage. Only in 2.5% of the left hemispheres was the sulcus of Jensen located anterior to the first caudal branch of the superior temporal sulcus.

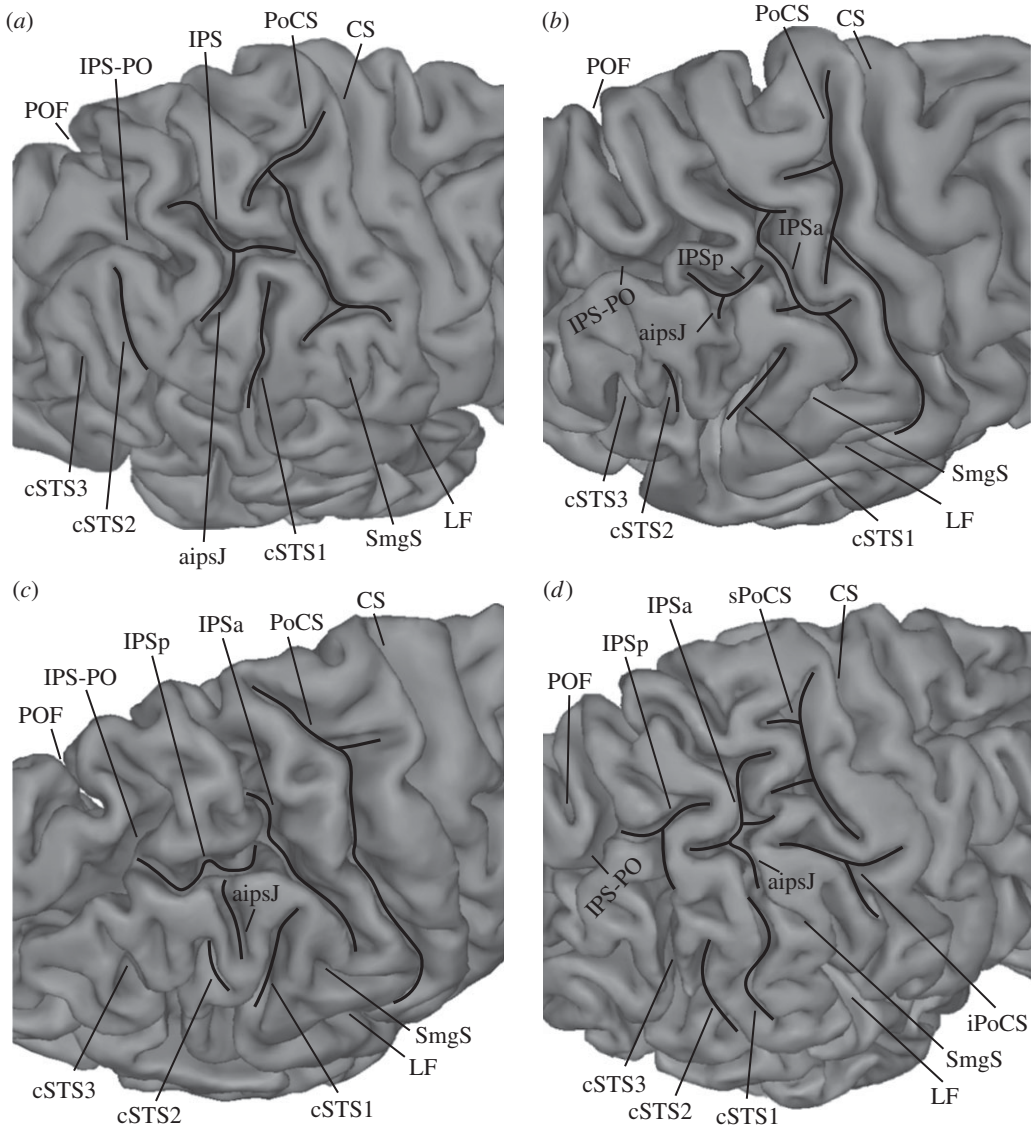

Figure 2. Demonstration of the anterior intermediate parietal sulcus of Jensen (aipsJ) in the hemispheres of different subjects. (*a*) aipsJ is clearly a downward branch of the intraparietal sulcus (IPS); (*b*) aipsJ is a simple notch; (*c*) aipsJ is a shallow sulcus merging with the IPS; (*d*) aipsJ connects superficially with the first caudal branch of the superior temporal sulcus (cSTS1). aipsJ, anterior intermediate parietal sulcus of Jensen; CS, central sulcus; cSTS1, first caudal branch of the superior temporal sulcus; cSTS2, second caudal branch of the superior temporal sulcus; cSTS3, third caudal branch of the superior temporal sulcus; iPoCS, inferior branch of the post-central sulcus; IPS, intraparietal sulcus (main horizontal part of the intraparietal sulcus); IPSa, anterior ramus of the horizontal part of the intraparietal sulcus; IPSp, posterior ramus of the horizontal part of the intraparietal sulcus; IPS-PO, paroccipital sulcus, often considered as the paroccipital part of the intraparietal sulcus; LF, lateral fissure; PoCS, post-central sulcus; POF, parietooccipital fissure; SmgS, supramarginal sulcus; sPoCS, superior branch of the post-central sulcus.

In 42.5% of the left hemispheres, the sulcus of Jensen and both rami of the IPS could be clearly identified. In 32.5% of these left hemispheres, the sulcus of Jensen was associated with the anterior ramus of the IPS. In 55% of the right hemispheres, both rami of the IPS and the sulcus of Jensen were observed. In these cases, the sulcus of Jensen was associated with either the anterior (27.5% of the right hemispheres; figure 2*d*; electronic supplementary material, figure S1*d*) or the posterior ramus of the IPS (27.5% of the right hemispheres; figure 2*b*,*c*; electronic supplementary material, figure S1*b*). When the sulcus of Jensen was associated with the posterior ramus of the IPS, it was located posterior to the gyral passage separating the anterior ramus from the posterior ramus of the IPS.

Note that in a few of the 80 hemispheres examined (5% of the left and 7.5% of the right hemispheres) the classification of the sulcus of Jensen was ambiguous, and therefore these cases were excluded when calculating the percentage of occurrence of this sulcus. In over a quarter of all examined hemispheres, a shallow sulcus or a set of dimples not connected with the IPS was observed between the first and second caudal branches of the superior temporal sulcus (27.5% of the left and 37.5% of the right hemispheres; figure 2*a*,*d*; electronic supplementary material, figure S1*e*).

4. Discussion

This study investigated the morphological variations of the IPS and the sulcus of Jensen, as well as how the latter sulcus relates to the three caudal branches of the superior temporal sulcus that invade the inferior parietal lobule and approach the IPS. Examination of the depth of the sulci based on a continuous series of sections demonstrated a number of novel facts. First, despite notable interindividual variability, the IPS can be clearly divided into two main parts (an anterior and a posterior ramus) by a gyral passage

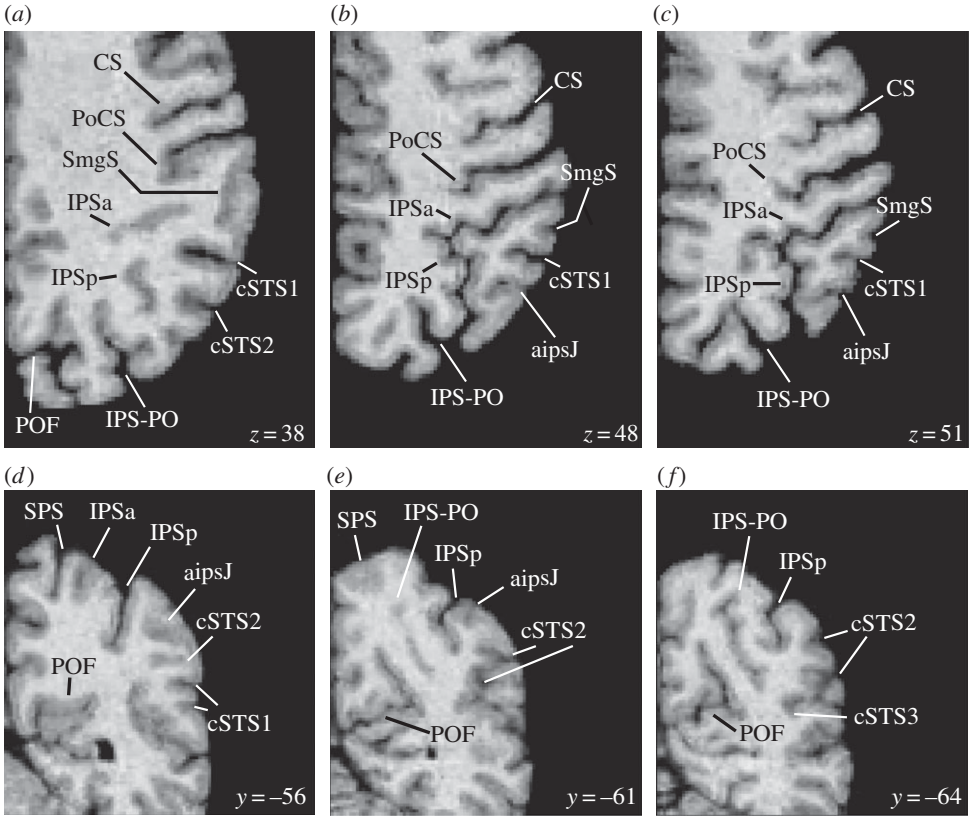

Figure 3. Horizontal and coronal sections from the right hemisphere of one subject showing two rami of the intraparietal sulcus (IPS) and the anterior intermediate parietal sulcus of Jensen (aipsJ). (*a–c*) Horizontal sections. The level in the dorsoventral dimension (*z*-coordinate) is provided in millimetres for each section. (*d–f*) Coronal sections. The level in the anterior–posterior dimension (*y*-coordinate) is provided in millimetres for each section. aipsJ, anterior intermediate parietal sulcus of Jensen; CS, central sulcus; cSTS1, first caudal branch of the superior temporal sulcus; cSTS2, second caudal branch of the superior temporal sulcus; cSTS3, third caudal branch of the superior temporal sulcus; IPSa, anterior ramus of the horizontal part of the intraparietal sulcus; IPSp, posterior ramus of the horizontal part of the intraparietal sulcus; IPS-PO, paroccipital sulcus, often considered as the paroccipital part of the intraparietal sulcus; PoCS, post-central sulcus; POF, parietooccipital fissure; SmgS, supramarginal sulcus; SPS, superior parietal sulcus.

that is either submerged (figures 2*b*,*c*, 3*a*; electronic supplementary material, figures S1*d*, S2, S4) or visible from the surface of the brain (figure 2*d*) in the majority of cerebral hemispheres. This subdivision of the IPS proper into two rami should not be confused with the distinction made by Ono *et al.* [37] between the IPS proper and the paroccipital sulcus (e.g. see figure on p. 67 in [37]; see also Results section of this article). The paroccipital sulcus is an independent sulcus that is sometimes referred to as a branch of the IPS [34]. As demonstrated here, in over half of all cases, the posterior ramus of the IPS and the paroccipital sulcus are clearly separated by a gyral passage visible from the surface of the brain (figure 2*a*,*b*; electronic supplementary material, figure S1*b*,*e*). Second, this study demonstrated three main patterns of the relation between the sulcus of Jensen and the IPS. The sulcus of Jensen emerges out of the inferior bank of the IPS, most frequently as a deep inferiorly directed branch of the IPS (figure 2*a*; electronic supplementary material, figure S1*a*, S3*a*); less frequently, it appears as a notch (figure 2*b*; electronic supplementary material, figure S1*b*, S3*b*) or a shallow sulcus merging with the IPS (figures 2*c*, 3; electronic supplementary material, figure S1*c*,*d*, S3*c*, S4–S8). Third, the relationship of the sulcus of Jensen with the three caudal branches of the superior temporal sulcus that invade the inferior parietal lobule and approach the IPS was defined. Most commonly, the sulcus of Jensen is located between the first and second caudal branches of the superior temporal sulcus, but in some hemispheres it connects superficially with the termination of the first caudal branch of the superior temporal sulcus (7.5% of the left and 17.5% of the right hemispheres; figure 2*d*; electronic supplementary material, figures S1*e*, S3*d*). In such cases, failure to examine continuous serial sections in detail and identify the first caudal branch of the superior temporal sulcus in the inferior parietal lobule (for instance, see [37, p. 16]) can lead to confusion of the caudalmost part of the first branch of the superior temporal sulcus with the sulcus of Jensen (for instance, see fig. 9.10C on p. 71 in [37]), which might have important functional consequences. Finally, the availability of the anatomical data in the MNI stereotaxic space [34] has allowed us to relate the morphological findings to functional neuroimaging data, which is impossible to do with data that are not presented in the standard stereotaxic space. The functional significance of the main morphological findings of this study is discussed below.

(a) The anterior and the posterior rami of the IPS may be the homologues in the human brain of areas AIP and LIP/PRR originally defined in the macaque monkey brain

A major finding of this study has been the demonstration that, in the majority of cases, the IPS consists of two main rami and, furthermore, that the anterior ramus extends anterior to the sulcus of Jensen, whereas the posterior ramus extends posterior to it. In the macaque monkey,

electrophysiological studies have identified a number of functional regions on the banks and fundus of the IPS, which are often referred to as the anterior, lateral and caudal intraparietal areas [49]. The anterior intraparietal area (AIP) is located in the anterior part of the IPS and its neuronal activity has been linked to grasping with the hand [3–5]. By contrast, neurons in the lateral intraparietal area (LIP), which is located on the lateral bank of the IPS posterior to area AIP, have saccade-related activity, including ongoing and anticipated saccades, and their activity is modulated by visual attention [6–8,10,13–14]. The posterior reach region (PRR) is located posteromedial to area LIP in the medial bank of the IPS and it is involved in reaching arm movements [10–11]. The limited available evidence suggests that the border between the AIP and LIP regions in the macaque monkey may be placed at the same anteroposterior level as the border between areas PF/PFG and PG (or area 7b, corresponding to PF/PFG, and area 7a, corresponding to area PG, in an older terminology used in macaque monkey studies) on the free surface of the inferior parietal lobule [50–53]. A systematic investigation combining single-cell recording in areas AIP and LIP with cytoarchitectonic analysis conducted in the same animals would be necessary to confirm this relation.

In the human brain, the cortex within the anterior ramus of the IPS, which lies anterior to the sulcus of Jensen and forms the medial border of areas PF/PFG of the supramarginal gyrus [36], may be the homologue of area AIP. By contrast, the posterior ramus, which lies posterior to the sulcus of Jensen and forms the medial border of area PG [36], may be the homologue of area LIP. The human homologue of area PRR may include the cortical region medial to the posterior ramus of the IPS, extending as far as the parietooccipital fissure. Thus, the sulcus of Jensen may be an important division of the anterior intraparietal sulcal cortex, processing information related to high-level sensorimotor control and the cortex within the posterior IPS contributing to visuospatial attentional processing. The available functional neuroimaging data discussed below are consistent with the above proposal.

The issue of the cortical topography of the homologues of areas AIP, PRR and LIP in the human brain has been addressed in functional neuroimaging studies investigating activation foci in the parietal cortex during the performance of hand movements (grasping, reaching or pointing), saccadic eye movements and visuospatial attentional processes [16–24,54–60] (for reviews, see [25–27]; also see electronic supplementary material, tables S1–S3). We projected the average coordinates of the putative AIP, LIP and PRR activity reported in these functional neuroimaging studies onto an average brain template (ICBM152 nonlinear sixth-generation model [48]) and examined the location of the peaks with respect to the IPS morphology as established in this study. Functional activity related to saccadic eye movements and attentional processing, reflecting putative area LIP, and activity related to pointing and reaching hand movements in the putative area PRR were observed in the posterior ramus of the IPS that lies caudal to the sulcus of Jensen. By contrast, activity related to grasping hand movements, reflecting putative area AIP, was located in the anterior ramus of the IPS (anterior to the sulcus of Jensen) and close to the junction of the IPS with the post-central sulcus, not only in the average-group data [24,56] (also see table 1 in [21] and table 1 in [22]), but also consistently observed in the individual subjects (see fig. 4 in [21]; [22–23]). Shikata *et al*. [22] localize the AIP homologue in the human brain at $x = -39.6$, $y = -40.1$, $z = 44.7$ and $x = 41.2$, $y = -40.6$, $z = 50.2$ (MNI space), and similar coordinates have been provided by Marangon *et al*. [24] ($x = -42.2$, $y = -43.1$, $z = 51.7$ and $x = 38.7$, $y = -35.7$, $z = 44.8$). These coordinates place the activity close to the gyral passage separating the post-central sulcus from the anterior ramus of the IPS [38]. If the narrow gyral passage is visible from the surface of the brain (figure 2*b–d*), then the activity appears to be located within the inferior branch of the post-central sulcus, located ventral to the IPS and the anterior ramus of the IPS. When this gyral passage is submerged (figure 2*a*), the functional activity may be found at the intersection of the post-central sulcus and the IPS, and may extend anteroventrally into the inferior branch of the post-central sulcus. Thus, it remains for future research to establish whether parts of the homologue of area AIP in the human brain may extend to the cortex within the inferior branch of the post-central sulcus.

Of particular interest is a neuroimaging experiment [20] that used the same saccade paradigm both in humans and macaque monkeys, namely the species in which area LIP has been defined physiologically. The results suggested a functional correspondence between the dorsal subdivision of area LIP in the monkey with the posterior IPS region in the human brain [20]. When we projected the MNI space coordinates reported by Koyama *et al*. [20] in the human subjects ($x = -22$, $y = -62$, $z = 60$ and $x = 22$, $y = -62$, $z = 60$) onto an average brain template (ICBM152 nonlinear sixth-generation model [48]), we observed that this putative homologue of area LIP in the human brain occurs close to the posterior ramus of the IPS near the inferior termination of the superior parietal sulcus. Other neuroimaging investigations consistently point to the posterior ramus of the IPS (i.e. posterior to the sulcus of Jensen) in the vicinity of the ventralmost point of the superior parietal sulcus as the locus of activation related to saccades, potentially reflecting putative area LIP [17,19,22,54,58] (see also electronic supplementary material, tables S1, S2). However, we must emphasize here that the detailed relations between sulcal morphology and LIP and PRR can only be understood from future studies that should explicitly examine such relations at the individual subject level in the context of individual morphological variation [28–30]. The anatomical findings of this study are a necessary prerequisite for such an examination.

Functional neuroimaging research suggests that the homologue of PRR in the human brain may involve, as in the macaque monkey, the superior parietal lobule, including the adjacent cortex in the IPS and the parietooccipital fissure [18,19,59–61] (for review, see [27]; also see electronic supplementary material, tables S2, S3). There is evidence that on the lateral surface of the posterior parietal cortex neural networks involved in planning and execution of saccades (putative area LIP homologue) and reaching and pointing hand movements (putative PRR homologue) overlap significantly; suggesting the absence of distinct effector-specific regions (see electronic supplementary material, table S2, and compare electronic supplementary material, tables S1, S3). Based on the descriptions and stereotaxic space coordinates provided in the literature (see electronic supplementary material, tables S2, S3), the human homologue of PRR may be located on the medial bank of the posterior ramus of the IPS and also medial to it in the superior parietal lobule. Although the individual-subject analysis by Bernier & Grafton [59] and Medendorp *et al*. [58] demonstrated that the putative homologue of PRR is located 'within a small sulcus running medially from the intraparietal sulcus' [58, p. 6211]

or 'slightly dorsal to the medial branch of IPS' [59, p. 778], future morphological examination of the superior parietal region is necessary to establish whether the sulcus the authors are referring to is an independent sulcus, such as the superior parietal sulcus, or a part of the IPS complex extending into the superior parietal lobule.

The available evidence in the monkey suggests that the posterior border of area LIP with area CIP is located in the most posterior part of the IPS before it merges with the lunate and parietooccipital sulci [12,15]. In the human brain, Shikata *et al.* [22] localize the intraparietal region involved in saccadic eye movements (putative area LIP) at $x = -25.6$, $y = -57$, $z = 58.4$ and $x = 26.1$, $y = -59.4$, $z = 57.6$. These MNI space coordinates would place LIP in the posterior ramus of the IPS as defined in this study. Area CIP in the human brain has been placed by Shikata *et al.* [22, pp. 416, 419] in a so-called 'side branch of the posterior intraparietal sulcus' anterior to the parietooccipital fissure. The MNI space coordinates ($x = -15.5$, $y = -66.3$, $z = 58.4$ and $x = 21$, $y = -65.7$, $z = 55.9$) and fig. 2 (p. 415) provided by Shikata *et al.* [22] allowed us to interpret the 'side branch of the posterior intraparietal sulcus' as the sulcus of Brissaud. This sulcus appears at the intersection of the posterior end of the IPS and the paroccipital sulcus, and therefore the available information localizes the putative area CIP in the human brain to this intersection of the posterior end of the IPS with the paroccipital sulcus (figure 1). We therefore interpret the data provided by Shikata *et al.* [22] for the human homologue of area LIP to be the posterior ramus of the IPS until its connection with the paroccipital sulcus. Beyond this point starts the CIP region. This is consistent with the suggestion by Orban *et al.* [62] that the human LIP homologue lies in the IPS until its confluence with the parietooccipital fissure, and therefore, according to the current morphological findings, it would consist of the posterior ramus of the IPS and its confluence with the paroccipital sulcus.

Data accessibility. Human MRI brain scans from the International Consortium for Brain Mapping (ICBM) database used in this article are disseminated by the Laboratory of Neuro Imaging at the University of Southern California (http://www.loni.usc.edu/). The identification numbers of the MRI scans are provided in the Methods section of this article.

Acknowledgements. We thank Meghan Butters, Jennifer Novek and Kai Xi Wang for help with the preparation of illustrations.

Funding statement. This study was supported by the Canadian Institutes of Health Research (CIHR) grant no. MOP-130361 to M.P. The brain MRI data for this project was provided by the International Consortium for Brain Mapping (ICBM; Principal Investigator: John Mazziotta, MD, PhD). ICBM funding was provided by the National Institute of Biomedical Imaging and BioEngineering.

References

1. Turner W. 1866 The convolutions of the human cerebrum topographically considered. Edinburgh, UK: Maclachlan & Stewart.
2. Taira M, Mine S, Georgopoulos AP, Murata A, Sakata H. 1990 Parietal cortex neurons of the monkey related to the visual guidance of hand movement. *Exp. Brain Res.* **83**, 29–36. (doi:10.1007/BF00232190)
3. Sakata H, Taira M, Murata A, Mine S. 1995 Neural mechanisms of visual guidance of hand action in the parietal cortex of the monkey. *Cereb. Cortex* **5**, 429–438. (doi:10.1093/cercor/5.5.429)
4. Murata A, Gallese V, Luppino G, Kaseda M, Sakata H. 2000 Selectivity for the shape, size, and orientation of objects for grasping in neurons of monkey parietal area AIP. *J. Neurophysiol.* **83**, 2580–2601.
5. Baumann MA, Fluet MC, Scherberger H. 2009 Context-specific grasp movement representation in the macaque anterior intraparietal area. *J. Neurosci.* **29**, 6436–6448. (doi:10.1523/JNEUROSCI.5479-08.2009)
6. Blatt GJ, Andersen RA, Stoner GR. 1990 Visual receptive field organization and cortico-cortical connections of the lateral intraparietal area (area LIP) in the macaque. *J. Comp. Neurol.* **299**, 421–445. (doi:10.1002/cne.902990404)
7. Barash S, Bracewell RM, Fogassi L, Gnadt JW, Andersen RA. 1991 Saccade-related activity in the lateral intraparietal area. I. Temporal properties; comparison with area 7a. *J. Neurophysiol.* **66**, 1095–1108.
8. Barash S, Bracewell RM, Fogassi L, Gnadt JW, Andersen RA. 1991 Saccade-related activity in the lateral intraparietal area II. Spatial properties. *J. Neurophysiol.* **66**, 1109–1124.
9. Shikata E, Tanaka Y, Nakamura H, Taira M, Sakata H. 1996 Selectivity of the parietal visual neurones in 3D orientation of surface of stereoscopic stimuli. *Neuroreport* **7**, 2389–2394. (doi:10.1097/00001756-199610020-00022).
10. Snyder LH, Batista AP, Andersen RA. 1997 Coding of intention in the posterior parietal cortex. *Nature* **386**, 167–170. (doi:10.1038/386167a0)
11. Batista AP, Buneo CA, Snyder LH, Andersen RA. 1999 Reach plans in eye-centered coordinates. *Science* **285**, 257–260. (doi:10.1126/science.285.5425.257)
12. Tsutsui K, Jiang M, Yara K, Sakata H, Taira M. 2001 Integration of perspective and disparity cues in surface-orientation-selective neurons of area CIP. *J. Neurophysiol.* **86**, 2856–2867.
13. Eskandar EN, Assad JA. 2002 Distinct nature of directional signals among parietal cortical areas during visual guidance. *J. Neurophysiol.* **88**, 1777–1790.
14. Bisley JW, Goldberg ME. 2003 Neuronal activity in the lateral intraparietal area and spatial attention. *Science* **299**, 81–86. (doi:10.1126/science.1077395)
15. Tsutsui K, Jiang M, Sakata H, Taira M. 2003 Short-term memory and perceptual decision for three-dimensional visual features in the caudal intraparietal sulcus (area CIP). *J. Neurosci.* **23**, 5486–5495.
16. Binkofski F, Dohle C, Posse S, Stephan KM, Hefter H, Seitz RJ, Freund HJ. 1998 Human anterior intraparietal area subserves prehension: a combined lesion and functional MRI activation study. *Neurology* **50**, 1253–1259. (doi:10.1212/WNL.50.5.1253)
17. Corbetta M *et al.* 1998 A common network of functional areas for attention and eye movements. *Neuron* **21**, 761–773. (doi:10.1016/S0896-6273(00)80593-0)
18. Connolly JD, Goodale MA, Desouza JF, Menon RS, Vilis T. 2000 A comparison of frontoparietal fMRI activation during anti-saccades and anti-pointing. *J. Neurophysiol.* **84**, 1645–1655.
19. Astafiev SV, Shulman GL, Stanley CM, Snyder AZ, Van Essen DC, Corbetta M. 2003 Functional organization of human intraparietal and frontal cortex for attending, looking, and pointing. *J. Neurosci.* **23**, 4689–4699.
20. Koyama M, Hasegawa I, Osada T, Adachi Y, Nakahara K, Miyashita Y. 2004 Functional magnetic resonance imaging of macaque monkeys performing visually guided saccade tasks: comparison of cortical eye fields with humans. *Neuron* **41**, 795–807. (doi:10.1016/S0896-6273(04)00047-9)
21. Frey SH, Vinton D, Norlund R, Grafton ST. 2005 Cortical topography of human anterior intraparietal cortex active during visually guided reaching. *Cogn. Brain Res.* **23**, 397–405. (doi:10.1016/j.cogbrainres.2004.11.010)
22. Shikata E, McNamara A, Sprenger A, Hamzei F, Glauche V, Büchel C, Binkofski F. 2008 Localization of human intraparietal areas AIP, CIP, and LIP using surface orientation and saccadic eye movement tasks. *Hum. Brain Mapp.* **29**, 411–421. (doi:10.1002/hbm.20396)
23. Cavina-Pratesi C, Monaco S, Fattori P, Galletti C, McAdam TD, Quinlan DJ, Goodale MA, Culham JC. 2010 Functional magnetic resonance imaging reveals the neural substrates of arm transport and

grip formation in reach-to-grasp actions in humans. *J. Neurosci.* **30**, 10 306–10 323. (doi:10.1523/JNEUROSCI.2023-10.2010)

24. Marangon M, Jacobs S, Frey SH. 2011 Evidence for context sensitivity of grasp representations in human parietal and premotor cortices. *J. Neurophysiol.* **105**, 2536–2546. (doi:10.1152/jn.00796.2010)
25. Culham JC, Valyear KF. 2006 Human parietal cortex in action. *Curr. Opin. Neurobiol.* **16**, 205–212. (doi:10.1016/j.conb.2006.03.005)
26. Medendorp WP, Buchholz VN, Van Der Werf J, Leoné F. 2011 Parietofrontal circuits in goal-oriented behaviour. *Eur. J. Neurosci.* **33**, 2017–2027. (doi:10.1111/j.1460-9568.2011.07701.x)
27. Vesia M, Crawford JD. 2012 Specialization of reach function in human posterior parietal cortex. *Exp. Brain Res.* **221**, 1–18. (doi:10.1007/s00221-012-3158-9)
28. Amiez C, Kostopoulos P, Champod A-S, Petrides M. 2006 Local morphology predicts functional organization of the dorsal premotor region in the human brain. *J. Neurosci.* **26**, 2724–2731. (doi:10.1523/JNEUROSCI.4739-05.2006)
29. Segal E, Petrides M. 2013 Functional activation during reading in relation to the sulci of the angular gyrus region. *Eur. J. Neurosci.* **38**, 2793–2801. (doi:10.1111/ejn.12277)
30. Amiez C, Petrides M. 2014 Neuroimaging evidence of the anatomo-functional organization of the human cingulate motor areas. *Cereb. Cortex* **24**, 563–578. (doi:10.1093/cercor/bhs329)
31. Cunningham DJ. 1892 *Contribution to the surface anatomy of the cerebral hemispheres by D. J. C., with a chapter upon cranio-cerebral topography by Victory Horsley*. Dublin, Ireland: Royal Irish Academy.
32. Retzius G. 1896 *Das Menschenhirn; Studien in der makroskopischen Morphologie*. Stockholm, Sweden: Norstedt and Soener.
33. Connolly CJ. 1950 *External morphology of the primate brain*. Springfield, IL: Charles C Thomas.
34. Petrides M. 2012 *The human cerebral cortex. An MRI atlas of the sulci and gyri in MNI stereotaxic space*. New York, NY: Academic Press.
35. Jensen J. 1870 *Die Furchen und Windungen der menschlichen Grosshirn-Hemisphären*. Druck und Verlag von Georg Reimer.
36. Economo C, Koskinas GN. 1925 *Die Cytoarchitektonik der Hirnrinde des erwachsenen Menschen*. Vienna, Austria: Springer.
37. Ono M, Kubik S, Abernathey CD. 1990 *Atlas of the cerebral sulci*. New York, NY: Georg Thieme Verlag, Thieme Medical Publishers.
38. Zlatkina V, Petrides M. 2010 Morphological patterns of the postcentral sulcus in the human brain. *J. Comp. Neurol.* **518**, 3701–3724. (doi:10.1002/cne.22418)
39. Mazziotta JC, Toga AW, Evans A, Fox PT, Lancaster JL. 1995 A probabilistic atlas of the human brain: theory and rationale for its development. *Neuroimage* **2**, 89–101. (doi:10.1006/nimg.1995.1012)
40. Mazziotta JC, Toga AW, Evans A, Fox PT, Lancaster JL. 1995 Digital brain atlases. *Trends Neurosci.* **18**, 210–211. (doi:10.1016/0166-2236(95)93904-C)
41. Mazziotta J *et al*. 2001 A probabilistic atlas and reference system for the human brain: International Consortium for Brain Mapping (ICBM). *Phil. Trans. R. Soc. B* **356**, 1293–1322. (doi:10.1098/rstb.2001.0915)
42. Sled JG, Zijdenbos AP, Evans AC. 1998 A non-parametric method for automatic correction of intensity non-uniformity in MRI data. *IEEE Trans. Med. Imaging* **17**, 87–97. (doi:10.1109/42.668698)
43. Collins DL, Neelin P, Peters TM, Evans AC. 1994 Automatic 3D intersubject registration of MR volumetric data in standardized Talairach space. *J. Comput. Assist. Tomogr.* **18**, 192–205. (doi:10.1097/00004728-199403000-00005)
44. MacDonald D. 1996 *Program for display and segmentation of surfaces and volumes*. Montreal, Canada: McConnell Brain Imaging Center, Montreal Neurological Institute. (Software available from http://www.bic.mni.mcgill.ca.)
45. Ad-Dab'bagh Y *et al*. 2006 The CIVET image-processing environment: a fully automated comprehensive pipeline for anatomical neuroimaging research. See http://www.bic.mni.mcgill.ca/users/yaddab/Yasser-HBM2006-Poster.pdf.
46. Van Essen DC. 2005 A population-average, landmark- and surface-based (PALS) atlas of human cerebral cortex. *Neuroimage* **28**, 635–662. (doi:10.1016/j.neuroimage.2005.06.058)
47. Talairach J, Tournoux P. 1988 *Co-planar stereotaxic atlas of the human brain: 3-dimensional proportional system: an approach to cerebral imaging*. Stuttgart, Germany: Thieme Medical Publishers.
48. Grabner G, Janke AL, Budge MM, Smith D, Pruessner J, Collins DL. 2006 Symmetric atlasing and model based segmentation: an application to the hippocampus in older adults. *Med. Image Comput. Comput. Assist. Interv.* **9**, 58–66. (doi:10.1007/11866763_8)
49. Grefkes C, Fink GR. 2005 The functional organization of the intraparietal sulcus in humans and monkeys. *J. Anat.* **207**, 3–17. (doi:10.1111/j.1469-7580.2005.00426.x)
50. Andersen RA, Asanuma C, Essick G, Siegel RM. 1990 Corticocortical connections of anatomically and physiologically defined subdivisions within the inferior parietal lobule. *J. Comp. Neurol.* **296**, 65–113. (doi:10.1002/cne.902960106)
51. Durand JB, Nelissen K, Joly O, Wardak C, Todd JT, Norman JF, Janssen P, Vanduffel W, Orban GA. 2007 Anterior regions of monkey parietal cortex process visual 3D shape. *Neuron* **55**, 493–505. (doi:10.1016/j.neuron.2007.06.040)
52. Gharbawie OA, Stepniewska I, Qi H, Kaas JH. 2011 Multiple parietal-frontal pathways mediate grasping in macaque monkeys. *J. Neurosci.* **31**, 11 660–11 677. (doi:10.1523/jneurosci.1777-11.2011)
53. Nelissen K, Borra E, Gerbella M, Rozzi S, Luppino G, Vanduffel W, Rizzolatti G, Orban GA. 2011 Action observation circuits in the macaque monkey cortex. *J. Neurosci.* **31**, 3743–3756. (doi:10.1523/jneurosci.4803-10.2011)
54. Sereno MI, Pitzalis S, Martinez A. 2001 Mapping of contralateral space in retinotopic coordinates by a parietal cortical area in humans. *Science* **294**, 1350–1354. (doi:10.1126/science.1063695)
55. Peeters R, Simone L, Nelissen K, Fabbri-Destro M, Vanduffel W, Rizzolatti G, Orban GA. 2009 The representation of tool use in humans and monkeys: common and uniquely human features. *J. Neurosci.* **29**, 11 523–11 539. (doi:10.1523/JNEUROSCI.2040-09.2009)
56. Jacobs S, Danielmeier C, Frey SH. 2010 Human anterior intraparietal and ventral premotor cortices support representations of grasping with the hand or a novel tool. *J. Cogn. Neurosci.* **22**, 2594–2608. (doi:10.1162/jocn.2009.21372)
57. Gallivan JP, McLean DA, Valyear KF, Pettypiece CE, Culham JC. 2011 Decoding action intentions from preparatory brain activity in human parieto-frontal networks. *J. Neurosci.* **31**, 9599–9610. (doi:10.1523/jneurosci.0080-11.2011)
58. Medendorp WP, Goltz HC, Vilis T, Crawford JD. 2003 Gaze-centered updating of visual space in human parietal cortex. *J. Neurosci.* **23**, 6209–6214.
59. Bernier PM, Grafton ST. 2010 Human posterior parietal cortex flexibly determines reference frames for reaching based on sensory context. *Neuron* **68**, 776–788. (doi:10.1016/j.neuron.2010.11.002)
60. Beurze SM, Toni I, Pisella L, Medendorp WP. 2010 Reference frames for reach planning in human parietofrontal cortex. *J. Neurophysiol.* **104**, 1736–1745. (doi:10.1152/jn.01044.2009)
61. Leoné FT, Heed T, Toni I, Medendorp WP. 2014 Understanding effector selectivity in human posterior parietal cortex by combining information patterns and activation measures. *J. Neurosci.* **34**, 7102–7112. (doi:10.1523/jneurosci.5242-13.2014)
62. Orban GA, Claeys K, Nelissen K, Smans R, Sunaert S, Todd JT, Wardak C, Durand J-B, Vanduffel W. 2006 Mapping the parietal cortex of human and non-human primates. *Neuropsychologia* **44**, 2647–2667. (doi:10.1016/j.neuropsychologia.2005.11.001)